

Exosomes deep sequencing identifies *miR-363-5p* as a non-invasive biomarker of axillary lymph node metastasis and prognosis in breast cancer

Xin Wang

Chinese Academy of Medical Science and Peking Union Medical College

Tianyi Qian

Chinese Academy of Medical Sciences & Peking Union Medical College Hospital of Skin Diseases and Institute of Dermatology

Siqi Bao

Wenzhou Medical University

Hengqiang Zhao

Chinese Academy of Medical Sciences & Peking Union Medical College Hospital of Skin Diseases and Institute of Dermatology

Hongyan Chen

Chinese Academy of Medical Science & Peking Union Medical College

Zeyu Xing

Chinese Academy of Medical Science & Peking Union Medical College

Yalun Li

Qindao University Medical College Affiliated Yantai Yuhuangding Hospital

Menglu Zhang

Chinese Academy of Medical Sciences and Peking Union Medical College

Xiangzhi Meng

Chinese Academy of Medical Sciences & Peking Union Medical College

Changchang Wang

Chinese Academy of Medical Sciences & Peking Union Medical College

Jie Wang

Chinese Academy of Medical Sciences & Peking Union Medical College

Hongxia Gao

Chinese Academy of Medical Sciences & Peking Union Medical College

Jiaqi Liu (✉ j.liu@cicams.ac.cn)

Chinese Academy of Medical Sciences Cancer Institute and Hospital <https://orcid.org/0000-0002-9775-2342>

Meng Zhou

Chinese Academy of Medical Sciences & Peking Union Medical College

Xiang Wang

Chinese Academy of Medical Sciences & Peking Union Medical College

Research article

Keywords: breast cancer, circulating exosome, lymph node metastasis, miRNA, miR-363-5p, PDGFB

Posted Date: March 9th, 2020

DOI: <https://doi.org/10.21203/rs.3.rs-16343/v1>

License:   This work is licensed under a Creative Commons Attribution 4.0 International License.

[Read Full License](#)

Abstract

Background: Breast cancer is the most common malignant tumor in females. Axillary lymph node (ALN) metastasis is an independent risk factor of prognosis and correlates with distant metastasis. However, the false-negative rate and complications of the standard procedure are not neglectable hitherto. It is necessary to develop an accurate non-invasive approach for lymph node staging.

Methods: In this study, circulating exosomal miRNA profiles in peripheral blood from 10 patients with breast cancer and 10 age-matched healthy women were obtained and analyzed using small RNA deep sequencing. Integrative profiles analysis and multiple cross-validation using in-house and external independent datasets were performed to evaluate the diagnostic performance. Functional assays were used to analyze cellular phenotypes and downstream targets of *miR-363-5p*.

Results: We found that the aberrant expression of exosomal *miR-363-5p* is significantly associated with tumorigenesis ($p=0.047$) and ALN metastasis ($p=0.019$). Serum exosomal *miR-363-5p* demonstrated the consistent down-regulated expression pattern in LN positive patients compared with LN negative patients across multiple independent datasets, which achieved high diagnostic performance in predicting lymph node metastasis (AUC=0.621-0.958). Furthermore, patients with a high expression level of *miR-363-5p* had significantly improved overall survival (HR=0.63, $\pm 95\%$ CI=0.45-0.89, $p=0.0075$). Functional experiments discovered that *miR-363-5p* acts by inhibiting the migration ability of breast cancer cells. Here we further identified Platelet Derived Growth Factor Subunit B (*PDGFB*) as a downstream target of *miR-363-5p*.

Conclusions: The *miR-363-5p* deficiency promoted metastasis via facilitating *PDGFB* expression, leading to overactivity of *PDGF* signaling in cancer cells. These results demonstrated that tumor metastasis is mediated by tumor-derived exosomes that affect cell growth signal regulation. Therefore, exosomal *miR-363-5p* may serve as a marker for ALN metastasis diagnosis in a non-invasive manner.

Introduction

Breast cancer is the most common malignant tumor in females with a global annual incidence of 266,120 (30%) and 40,920 (14%) deaths [1]. Axillary lymph node (ALN) metastasis is one of the most important independent risk factors of the prognosis of early breast cancer [2]. Sentinel lymph node biopsy (SLNB) and ALN dissection are two major procedures for the ALN status evaluation and treatment for ALN metastasis. Currently, SLNB is recommended as the standard approach for ALN evaluation in clinically node-negative breast cancer patients [3]. Although unnecessary axillary clearance procedures might be spared, sentinel lymph nodes could have a false negative rate of 7.3%, which leads to patient under-treatment and causes an increased risk of recurrence [4, 5]. Additionally, the presence of SLNB complications especially lymphedema is still inevitable. The incidence rate is 3.5% in breast cancer patients who received SLNB alone without ALN dissection [6]. And thus, it is highly necessary to develop an accurate and non-invasive method to identify patients at low risk of ALN metastasis before surgery.

Patients without ALN metastasis would benefit vastly if SLNB could be avoided safely using pre-surgery ALN status evaluation.

Exosomes are 30 to 100 nm microvesicles formed in multivesicular bodies and released into the extracellular environment by most cell types [7]. Abundant studies have shown that exosomes can serve as mediators of cell-to-cell communication by delivering cargo molecules especially nucleic acids that regulate the tumor microenvironment and promote cancer metastasis and progression [8-10]. Meanwhile, serum exosomes of cancer patients were proved to have a higher concentration than healthy individuals and considered as reliable markers in cancer diagnosis [11, 12]. Within the serum exosomes, there are stuffed with a selection of mRNAs, microRNAs (miRNAs), long non-coding RNAs (lncRNAs), proteins, and lipids [13]. The miRNAs are small non-coding RNAs that regulate the cellular process by suppressing target mRNA translation and present with a high level in an exosome [14]. Recent studies have shown that exosomal miRNAs exhibit essential biological effects on tumor metastasis [15, 16]. Besides, there is growing evidence suggesting the potential role of exosomal miRNAs in early detection of cancer metastasis [13, 17, 18]. However, the relation between tumor-derived exosomal miRNAs and the lymph node metastases in breast cancer is still unclear. Meanwhile, biomarkers based on serum exosomes for clinical applications were underdeveloped.

Here, we conducted a prior study to investigate the potential use of circulating exosomal miRNAs in the detection of lymph node metastasis (LNM). In this study, small RNA deep sequencing (RNAseq) analysis was used aiming to characterize the miRNA expression landscape in the serum exosomes from breast cancer patients. The candidate miRNAs responsible for breast cancer LNM were generated by comparing the miRNA expression difference between patients with or without LNM. Additionally, candidate miRNAs were verified in multiple independent patient datasets. Furthermore, *in silico* and experimental studies were performed to identify potentially relevant target genes of the candidate miRNA for improving our understanding of mechanisms underlying the LNM in breast cancer.

Materials And Methods

Patient enrollment and sample preparation

All participants were enrolled through the Genetic investigation of Inherited and Familial Tumor Syndrome (GIFTS) study between January 2018 and June 2018 from the Cancer Hospital, Chinese Academy of Medical Sciences (CHCAMS). Patients were eligible for enrollment if they had an evident histologic diagnosis of breast cancer and without distant metastasis. Age-matched healthy women were also recruited as a control group. Peripheral blood samples of 10ml from these breast cancer patients and ten age-matched healthy women were collected at CHCAMS. Blood samples were collected in vacuum tubes with EDTA and centrifugated at $3,000 \times g$ for 15 minutes at 4°C , the collected supernatant (5 ml plasma) was preserved at -80°C before use. All participants signed written informed consent. Ethics approval for the study was obtained from the Research Ethics Committee of CHCAMS.

Exosome isolation

The collected plasma was thawed at 37°C and then centrifugated at 3,000 ×g for 15 minutes to remove cell debris. Aspirated supernatant was diluted 7-fold with PBS and centrifuged at 13,000 ×g for 30 minutes [19]. Large particles were removed using 0.22 µm filters. Then the collected supernatant was ultra-centrifuged at 100,000 ×g, 4°C for 2 h (CP100NX; Hitachi, Brea, CA, USA). The pellet containing exosomes was re-suspended in PBS and ultra-centrifuged again at 100,000 ×g 4°C for 2 h. The isolated exosomes were re-suspended in 100 µl PBS after PBS washing for further analysis.

Exosomes Characterization

The nanoparticle tracking analysis (NTA), transmission electron microscopy (TEM), and western blot analysis using rabbit polyclonal antibody CD63, TSG101, and calnexin were conducted following the previously reported protocols [20].

Exosomal RNA isolation and RNA analyses

The RNAs were extracted from plasma-isolated exosomes using the miRNeasy® Mini kit (Qiagen, cat. No. 217004). RNA yields as well as DNA contamination were monitored on a 1.50% agarose gel. The NanoDrop 2000 spectrophotometer (Thermo Fisher Scientific, Wilmington, Germany) was used to assess RNA concentration and purity. The integrity and distribution of RNAs were analyzed using the Agilent Bioanalyzer 2100 system with RNA Nano 6000 Assay Kit (Agilent Technologies, CA, USA).

Library preparation and sequencing

First, a total amount of 5 ng RNA per sample was depleted of rRNA using the RiboZero magnetic kit (Epicentre, Madison, Wisconsin, USA). Then, the sequencing libraries were generated using the Ovation® RNA-Seq System (NuGEN, CA, USA). A total amount of 2.5 µg RNA per sample was used as input material for sample preparation of small RNA libraries. Then, the libraries were generated using the NEB Next Multiplex Small RNA Library Prep Set for Illumina (NEB, USA). The index codes were added to attribute sequences to each sample. Finally, the polymerase chain reaction (PCR) products were purified using the Agencourt Ampure XP system (Beckman Coulter, Brea, CA, USA). The the library quality was evaluated on an Agilent Bioanalyzer 2100 (Agilent Technologies, Palo Alto, CA, USA) and quantitative PCR. The cluster of the index-coded samples was generated by the acBot Cluster Generation System using TruSeq PE Cluster Kitv3-cBot-HS (Illumina, San Diego, CA). At last, the sequencing was performed on the Illumina Hiseq platform using the library preparations and paired-end reads were generated.

Quantitative differential expression analysis of miRNA

The sequence alignment was performed using the Bowtie tool [21] with several databases including the Silva database (<https://www.arb-silva.de/>), the GtRNADB database (<http://gtrnadb.ucsc.edu/>), the Rfam database (<http://rfam.sanger.ac.uk/>), and the Rfam database (<http://www.girinst.org/>) [22].

Subsequently, the rRNA, transfer RNA, small nuclear RNA, small nucleolar RNA, and other non-coding RNA were filtered. Then, the miRNA including known miRNAs and novel miRNAs were detected using the remaining reads, in which the novel miRNAs were predicted according to the miRbase database and

Human Genome (GRCh38), respectively. Read counts of the miRNAs were generated from the mapping results and have been standardized as the total mapped reads (TPM) per million. Circulating exosomal miRNA profiles of samples with two conditions were compared by the Student's t test (two-tailed), and each miRNAs with a $\log_2|\text{fold change}| > 0.58$ and $p < 0.05$ was considered as differential expression. Hierarchical clustering was performed with R package 'pheatmap' using the ward.D2 method.

Cell culture and transfection

The MCF-7 cell line was cultured at 37°C with 5% CO₂. Dulbecco's modified Eagle's medium (DMEM, SH30022.01, HyClone, South Logan, UT, USA) with 10% fetal bovine serum (FBS, FND500, ExCell Bio., Shanghai, China) was applied as culture medium. One hundred units per milliliter penicillin and 100 µg/ml streptomycin (SV30010, Hyclone, Logan, UT, USA) were also added into DMEM. Until the density reached approximately 50-70%, cells were transfected for 48 hours with miR-363-5p mimic, mock negative control (NC), miR-363-5p inhibitor or inhibitor NC (Ribo, Guangzhou, China) using Lipofectamine 2000 (Invitrogen, Carlsbad, CA, USA).

RNA extraction and quantification

The miRNA was extracted from MCF-7 cells with the miRcute miRNA isolation kit (DP501, Tiangen, China). Total RNA was extracted from transfected MCF-7 cells with the total RNA rapid extraction kit (China (220010, Feijie biological, China). After quality control, the FastQuant RT kit (KR106, China) was used to reverse transcribe the miRNA or RNA sample into cDNA. qRT-PCR was performed in an ABI 7300 real-time PCR system (Applied Biosystems, Foster City, California, USA). SuperReal PreMix Plus (SYBR Green) mixture (FP205, Tiangen, China) was applied for reactions. The relative amount of *miR-363-5p* to control *U6* and *PDGFB* to control GAPDH transcripts were analyzed by the $2^{-\Delta\Delta C_t}$ method. Primers applied were listed as follows: *miR-363-5p*: forward: 5'-CGGGTGGATCACGATG-3'; reverse: 5'-CAGTGCAGGGTCCGAGGTAT-3'; *U6*: forward: 5'-CTCGCTTCGGCAGCAC-3'; reverse: 5'-AACGCTTCACGAATTTGCGT-3' [23].

Cell proliferation assay

The MCF-7 cells were plated in 96-well plates with a density of 5×10^3 cells/well. The proliferation of cells at 0h, 24h, 48h, and 72 h after transfection was examined using the CCK-8 proliferation assay kit (MA2018-L, Meilunbio, China). Ten microliters of CCK-8 reagent was added to the medium at every time phase. Absorbance at 450nm was measured after 3 h incubation using microplate spectrometer reader (Molecular Devices, CA, USA).

Transwell migration assay

After transfection with *miR-363-5p* or NC for 48 h, MCF-7 cell was washed twice with FBS-free medium, and then re-suspended in FBS-free medium at a density of 1×10^5 cells/ml. Transwell chamber (pore size 8.0 µm, 3422, Corning Costar, MA, USA) pre-treated with the FBS-free medium was placed in a 24-well

plate. After removing the pre-treatment medium, the lower chamber was added with 600 μ L 10% FBS containing medium, while the upper chamber was added with 100 μ L cell suspension. After incubating for 48 h, the chambers were fixed and stained with methanol and 0.2% crystal violet. After staining, cells on the chamber surface were removed carefully with water and cotton swabs. The number of perforated cells in the outer layer of the basement membrane of each chamber (migrating cells) was counted in five random high power fields with phase-contrast microscope (NIB-100F, Novel, China).

Statistical analysis

Analyses were performed with R Statistical Software (version 3.5.3). Pre-set $p < 0.05$ was defined as statistically significant. Quantitative data were measured as mean \pm standard deviation. The comparison of mean values between two groups was analyzed using Student's t test and Mann-Whitney U-test. Pearson's test was used to evaluate the exosome-tissue miRNA correlation and miRNA-target mRNA correlation. Receiver Operating Characteristic (ROC) curve analysis was used to determine the diagnostic performance, and the area under the curve (AUC) were calculated with R package 'ROCit' [24]. Kaplan Meier method and log-rank test were applied to compare survival differences using R package 'Survival'.

Result

Characterization of exosomes from the serum of breast cancer patients

In this study, 10 breast cancer patients and 10 age-matched healthy women were enrolled. Clinical information of the patients was listed in Table 1. 10 breast cancer patients were further divided into two groups according to their lymph node status, namely four patients with LNM and six patients without LNM. Blood samples were collected from both breast cancer patients and healthy controls. The integrity of exosome preparation was confirmed with TEM followed by western blot. The exosomes isolated from the serum exhibited the classic cup-shaped morphology under TEM (Supplementary Fig. 1A). Exosome markers *TSG101* and *CD63* expression were detected from the exosome isolated from the serum (Supplementary Fig. 1B). The NTA indicated that the average size of the vesicles was 105.7nm, and the main peak of particle diameter was at 85.5nm (Supplementary Fig. 1C). The above-mentioned results demonstrated that the extracellular vesicles isolated from serum samples are purified exosomes.

RNA-seq identified dysregulated exo-miRNAs in breast cancer patients

To identify exo-miRNAs that play a pivotal role in inducing breast cancer LNM, circulating exosomal miRNAs were isolated and profiled using small RNA deep sequencing analysis. A total of 1631 miRNAs were mapped in exosomes isolated from serum samples. To minimize noise and improve accuracy, the miRNAs with TPM values less than 5 were removed, leaving 367 miRNAs for further analysis. Through differential expression analysis, 43 significantly differentially expressed (DE) miRNAs were identified in breast tumor exosomes and 7 significantly DE miRNAs in breast tumor exosomes with LN positive status. Fig. 1A shows a different expression pattern of the 43 DE miRNAs between healthy and breast cancer

patients. Fig. 1B shows a different expression pattern of the 7 DE miRNAs between breast cancer patients with and without LNM.

Identification of serum exosomal *miR-363-5p* as a potential biomarker of axillary lymph node metastasis and prognosis

Integrative profiles analysis indicated that the aberrant expression of exosomal *miR-363-5p* is significantly associated with both tumorigenesis ($p=0.047$) and ALN metastasis ($p=0.019$) (Fig. 2A). Exosomal *miR-363-5p* expression was significantly higher in breast cancer patients compared with healthy controls and was significantly lower in LN positive patients compared with LN negative patients (Fig. 2B). Since the miRNA concentration in exosomes is distinctively related to its cellular abundance [25], we also hypothesized that reliable circulating markers should coordinate with their expression alterations in tumor tissues. To verify the reliability of *miR-363-5p*, the expression levels of *miR-363-5p* in tumor tissues with LN positive and LN negative status were compared in four external independent datasets (i.e. three GEO datasets GSE38167, GSE31309, GSE42072, and The Cancer Genome Atlas [TCGA] dataset). The expression pattern of *miR-363-5p* in tumor tissues was identical to that in exosomes in in-house and four external independent datasets (Fig. 2C). Patients with LN positive status had a significantly lower *miR-363-5p* expression in GSE38167 ($p=0.013$), GSE31309 ($p=0.136$), GSE42072 ($p=0.123$) and TCGA ($p=0.014$) datasets. We subsequently profiled the expression levels of the miRNAs in tumor tissue of the 10 breast cancer patients (in-house data) using qRT-PCR. *miR-363-5p* expression in breast cancer tissue was significantly lower in LN positive patients (Fig. 2D). Additionally, our in-house data showed the exosomal concentrations of *miR-363-5p* correlated with its expression in tumor tissue (Pearson's $r=-0.679$ and $p=0.0307$, Fig. 2E). These validation analyses indicated the potential of *miR-363-5p* as a potential and stable non-invasive biomarker for further investigation

Performance evaluation and validation of *miR-363-5p* in the in-house set and multiple independent datasets

In order to retrospectively evaluate the predictive power of exosomal *miR-363-5p* on detecting LN metastasis, we performed ROC analysis and found that the *miR-363-5p* achieved high diagnostic performance with AUC of 0.958 for in-house data and 0.733, 0.621 and 0.639 in GSE38167, GSE31309, and GSE42072 (Fig. 3A), respectively. These results indicated that low *miR-363-5p* expression levels could be a new diagnostic marker for breast cancer LN metastasis. Furthermore, we assessed the association between *miR-363-5p* expression level and survival of breast cancer patients and found that patients with the low expression level of *miR-363* had significantly worse overall survival ($p=0.0075$, Fig. 3B). Moreover, in patients with negative lymph nodes upon the first diagnosis, low expression of *miR-363* in primary tumors correlates with the significantly worse outcome ($p=0.00094$, Fig. 3C). Survival analysis indicated that the downregulation of *miR-363* could serve as a prognostic marker of poor survival in breast cancer.

***miR-363-5p* inhibits metastatic properties of breast cancer cell**

The *miR-363-3p* and *miR-363-5p* (*miR-363**) are both the mature forms of *miR-363*. Previous studies have focused on the biological function and pathophysiological significance of *miR-363-3p*, but little explored the role of *miR-363-5p*, possibly because of its relatively low abundance compared with *miR-363-3p*. To investigate the role of circulating exosomal *miR-363-5p* in breast cancer progression, we hypothesized that *miR-363-5p* influence breast cancer cell mobility. We selected an ER-positive breast cancer cell line MCF-7, and transfected breast cancer cells with liposomal vectors overexpressing *miR-363-5p* or negative control (NC). Migration assays showed that overexpressing *miR-363-5p* significantly represses migration ability and silencing *miR-363-5p* results in intensified cell migration (Fig. 4A & Fig. 4B). The cell viability showed no significance in overexpression or knock-down of *miR-363-5p* (Fig. 4C).

Exosomal *miR-363-5p* modulates platelet-derived growth factor (PDGF) signaling activity by targeting *PDGFB*

To identify reliable targets of *miR-363-5p*, we utilized both experimentally validated miRNA-target interaction databases and co-expression analysis (Fig. 5A). We analyzed miRNA and mRNA expression profiles of the TCGA breast cancer dataset and yielded four mRNAs co-expressed with *miR-363-5p* based on the negative regulation of target gene expression and miRNA level. We also retrieved gene lists of experimentally established targets of *miR-363-5p* from two databases (mirTarbase and Tarbase). We merged the results from two databases and yielded a list of 234 target genes. Among them, *PDGFB* was the only one exhibiting a significant negative correlation (Pearson's $r=-0.208$, $p<0.001$) with the *miR-363-5p* level in breast cancer tissues from TCGA (Fig. 5B). The target location (Fig. 5C) was provided by the previous study, validated using PAR-CLIP [26]. Thus, it was selected as a potential target for further functional target characterization. We next performed the qRT-PCR for validation. Consistent with the bioinformatics analysis, qRT-PCR analysis also showed that *PDGFB* expression is significantly downregulated by *miR-363-5p* overexpression, which is subsequently rescued by *miR-363-5p* knockdown as well (Fig. 5D). These findings indicated that *miR-363-5p* regulates *PDGFB* expression in breast cancer. *miR-363-5p* deficiency promoted metastasis via facilitating *PDGFB* expression, leading to overactivity of PDGF signaling in cancer cells.

Discussion

Assessment of miRNA expression signatures in exosomes is a promising tool for cancer research and clinical diagnosis, here in this study we report the different miRNA signature and identified several deregulated miRNAs in breast cancer patients with ALN metastasis compared with those without ALN metastasis. We identified that the level of exosomal *miR-363-5p* in ALN positive breast cancer patients was significantly lower than that in ALN negative patients.

Evaluation of miRNA expression in tumor tissues is necessary since the parallel down-regulation acts as the logical foundation of a tumor-derived diagnostic marker, and indispensable for mechanism interpretation as well. We investigated *miR-363-5p* level in breast cancer tissue of both in-house patients and external datasets. The results were consistent with that of serum exosomes. Those patients who

were diagnosed with LN positive breast cancer have a significantly lower level of *miR-363-5p*. These results indicated that deregulated exosomal *miR-363-5p* level is associated with transcriptional changes in primary tumor tissue. And these changes substantially contribute to LNM in breast cancer.

We performed *in silico* diagnosis test and verified that *miR-363-5p* alone has an AUC of 0.621-0.958 in predicting LN metastasis in multiple independent datasets. Previous studies have shown that imaging approaches namely axillary ultrasound and MRI have similar performance in ALN staging, and the AUC of MRI alone was 0.665 [27, 28]. We deem that exosomal *miR-363-5p* can help elevate the accuracy of clinical prediction models if taken into consideration. Furthermore, survival analysis revealed that patients with lower *miR-363-5p* have a significantly worse prognosis, especially in node-negative patients at their initial diagnosis. This suggests that patient stratification using *miR-363-5p* can help distinguish individuals with a high risk of breast cancer death. Node-negative patients with low *miR-363-5p* level might consider adjuvant endocrine therapy.

In this study, we also investigated the functional significance of *miR-363-5p*. We found that restoration of *miR-363-5p* using mimics significantly inhibited breast cancer cell migration, while it seemed proliferation was not affected. Studies have revealed that low *miR-363* expression is associated with carcinogenesis and metastasis [29, 30]. Overexpression of *miR-106a-363* cluster (*miR20b*, *miR-363-3p* and *miR-363-5p*) exhibited an anti-proliferative effect on cancer cells[31]. Our data indicated that among them *miR-363-5p* does not cause proliferation changes, but only migration ability. The previous study constructed a prognosis model of node-negative patients mainly based on receptor status and tumor size[32]. MiRNA signature can provide distinct tumor information on its cellular and molecular characteristics and would increase the accuracy of clinical prediction models. Our functional study defined the basic rationale and supported *miR-363-5p* as a specific complementary predictor for LN metastasis as well as patient prognosis.

It has been reported that *miR-363-5p* modulates endothelial cell-specific genes including angiocrine factors [33], which is consistent with our result. We found that *miR-363-5p* regulates *PDGFB* by binding to its 3'-UTR, which inhibits the activation of PDGF/PDGFR-related pathways. It is reported that the metastatic potential of mammary epithelial cells depends on the PDGF-PDGFR loop [34]. PDGF autocrine activates *STAT1* and other pathways, contributing to the induction and maintenance of the EMT in breast cancer. *PDGFB* and dimer protein PDGF-BB is an important lymphangiogenic factor and contributes to cancer lymphatic metastasis by stimulating MAP kinase activity [35, 36]. *PDGFB* exhibited both proliferative and chemotactic effects on lymphatic endothelial cells and directly cause lymphatic metastasis in breast cancer bearing mice [37]. In summary, *miR-363-5p/PDGFB* might play a pivotal role in breast cancer carcinogenesis and progression, especially related to lymph node staging. Furthermore, *miR-363-5p* might represent a relatively downstream element in a complicated regulation network, different pathways involved in this process require further exploration.

Nevertheless, this study has several limitations as follows: 1) The present study only included ER+ HER2- patients and further verification is necessary for other molecular types; 2) The sample size of our

discovery cohort is relatively small;3) Accuracy of exosomal *miR-363-5p* alone is not enough and thus construction of an integrated model is required.

Conclusion

In conclusion, our study identified exosome miRNA markers that help evaluate LN status in a non-invasive manner. Exosomal *miR-363-5p* showed good accuracy and was confirmed with a functional and molecular basis. These results indicate that exosomal *miR-363-5p* may be applicable in developing liquid biopsy strategies to effectively diagnose LN metastasis in breast cancer.

References

1. Siegel RL, Miller KD, Jemal A: **Cancer statistics, 2018**. *CA Cancer J Clin* 2018, **68**(1):7-30.
2. Carter CL, Allen C, Henson DE: **Relation of tumor size, lymph node status, and survival in 24,740 breast cancer cases**. *Cancer* 1989, **63**(1):181-187.
3. Lyman GH, Somerfield MR, Bosserman LD, Perkins CL, Weaver DL, Giuliano AE: **Sentinel Lymph Node Biopsy for Patients With Early-Stage Breast Cancer: American Society of Clinical Oncology Clinical Practice Guideline Update**. *Journal of clinical oncology : official journal of the American Society of Clinical Oncology* 2017, **35**(5):561-564.
4. Kim T, Giuliano AE, Lyman GH: **Lymphatic mapping and sentinel lymph node biopsy in early-stage breast carcinoma: a metaanalysis**. *Cancer* 2006, **106**(1):4-16.
5. Pesek S, Ashikaga T, Krag LE, Krag D: **The false-negative rate of sentinel node biopsy in patients with breast cancer: a meta-analysis**. *World journal of surgery* 2012, **36**(9):2239-2251.
6. Langer I, Guller U, Berclaz G, Koechli OR, Schaer G, Fehr MK, Hess T, Oertli D, Bronz L, Schnarwyler B *et al*: **Morbidity of sentinel lymph node biopsy (SLN) alone versus SLN and completion axillary lymph node dissection after breast cancer surgery: a prospective Swiss multicenter study on 659 patients**. *Annals of surgery* 2007, **245**(3):452-461.
7. Théry C, Zitvogel L, Amigorena S: **Exosomes: composition, biogenesis and function**. *Nature reviews Immunology* 2002, **2**(8):569-579.
8. Mu W, Rana S, Zoller M: **Host matrix modulation by tumor exosomes promotes motility and invasiveness**. *Neoplasia (New York, NY)* 2013, **15**(8):875-887.
9. Luga V, Zhang L, Vitoria-Petit AM, Ogunjimi AA, Inanlou MR, Chiu E, Buchanan M, Hosein AN, Basik M, Wrana JL: **Exosomes mediate stromal mobilization of autocrine Wnt-PCP signaling in breast cancer cell migration**. *Cell* 2012, **151**(7):1542-1556.
10. Peinado H, Alečković M, Lavotshkin S, Matei I, Costa-Silva B, Moreno-Bueno G, Hergueta-Redondo M, Williams C, García-Santos G, Ghajar C *et al*: **Melanoma exosomes educate bone marrow progenitor cells toward a pro-metastatic phenotype through MET**. *Nature medicine* 2012, **18**(6):883-891.
11. Huang X, Yuan T, Liang M, Du M, Xia S, Dittmar R, Wang D, See W, Costello BA, Quevedo F *et al*: **Exosomal miR-1290 and miR-375 as prognostic markers in castration-resistant prostate cancer**. *Eur*

Urol 2015, **67**(1):33-41.

12. Melo SA, Luecke LB, Kahlert C, Fernandez AF, Gammon ST, Kaye J, LeBleu VS, Mittendorf EA, Weitz J, Rahbari N *et al*: **Glypican-1 identifies cancer exosomes and detects early pancreatic cancer.** *Nature* 2015, **523**(7559):177-182.
13. An T, Qin S, Xu Y, Tang Y, Huang Y, Situ B, Inal JM, Zheng L: **Exosomes serve as tumour markers for personalized diagnostics owing to their important role in cancer metastasis.** *J Extracell Vesicles* 2015, **4**:27522.
14. Valadi H, Ekstrom K, Bossios A, Sjostrand M, Lee JJ, Lotvall JO: **Exosome-mediated transfer of mRNAs and microRNAs is a novel mechanism of genetic exchange between cells.** *Nat Cell Biol* 2007, **9**(6):654-659.
15. Epstein DM: **Special delivery: microRNA-200-containing extracellular vesicles provide metastatic message to distal tumor cells.** *The Journal of clinical investigation* 2014, **124**(12):5107-5108.
16. Zhuang G, Wu X, Jiang Z, Kasman I, Yao J, Guan Y, Oeh J, Modrusan Z, Bais C, Sampath D *et al*: **Tumour-secreted miR-9 promotes endothelial cell migration and angiogenesis by activating the JAK-STAT pathway.** *EMBO J* 2012, **31**(17):3513-3523.
17. Feng C, She J, Chen X, Zhang Q, Zhang X, Wang Y, Ye J, Shi J, Tao J, Feng M *et al*: **Exosomal miR-196a-1 promotes gastric cancer cell invasion and metastasis by targeting SFRP1.** *Nanomedicine (Lond)* 2019.
18. Zhang Z, Li X, Sun W, Yue S, Yang J, Li J, Ma B, Wang J, Yang X, Pu M *et al*: **Loss of exosomal miR-320a from cancer-associated fibroblasts contributes to HCC proliferation and metastasis.** *Cancer Lett* 2017, **397**:33-42.
19. Wang Q, Han CL, Wang KL, Sui YP, Li ZB, Chen N, Fan SY, Shimabukuro M, Wang F, Meng FG: **Integrated analysis of exosomal lncRNA and mRNA expression profiles reveals the involvement of lnc-MKRN2-42:1 in the pathogenesis of Parkinson's disease.** *CNS Neurosci Ther* 2019.
20. Min L, Zhu S, Chen L, Liu X, Wei R, Zhao L, Yang Y, Zhang Z, Kong G, Li P *et al*: **Evaluation of circulating small extracellular vesicles derived miRNAs as biomarkers of early colon cancer: a comparison with plasma total miRNAs.** *J Extracell Vesicles* 2019, **8**(1):1643670.
21. Langmead B, Trapnell C, Pop M, Salzberg SL: **Ultrafast and memory-efficient alignment of short DNA sequences to the human genome.** *Genome Biol* 2009, **10**(3):R25.
22. Yang T, Ma H, Zhang J, Wu T, Song T, Tian J, Yao Y: **Systematic identification of long noncoding RNAs expressed during light-induced anthocyanin accumulation in apple fruit.** *Plant J* 2019, **100**(3):572-590.
23. Ying J, Yu X, Ma C, Zhang Y, Dong J: **MicroRNA-363-3p is downregulated in hepatocellular carcinoma and inhibits tumorigenesis by directly targeting specificity protein 1.** *Mol Med Rep* 2017, **16**(2):1603-1611.
24. Khan MRAA: **ROCit-An R Package for Performance Assessment of Binary Classifier with Visualization.** 2019.

25. Koppers-Lalic D, Hackenberg M, Bijnsdorp IV, van Eijndhoven MAJ, Sadek P, Sie D, Zini N, Middeldorp JM, Ylstra B, de Menezes RX *et al*: **Nontemplated nucleotide additions distinguish the small RNA composition in cells from exosomes.** *Cell Rep* 2014, **8**(6):1649-1658.
26. Hamilton MP, Rajapakshe KI, Bader DA, Cerne JZ, Smith EA, Coarfa C, Hartig SM, McGuire SE: **The Landscape of microRNA Targeting in Prostate Cancer Defined by AGO-PAR-CLIP.** *Neoplasia (New York, NY)* 2016, **18**(6):356-370.
27. Almeray T, Villacreses D, Li Z, Patel B, McDonough M, Gibson T, Maimone S, Gray R, McLaughlin SA: **Value of Axillary Ultrasound after Negative Axillary MRI for Evaluating Nodal Status in High-Risk Breast Cancer.** *Journal of the American College of Surgeons* 2019, **228**(5):792-797.
28. Liu Z, Feng B, Li C, Chen Y, Chen Q, Li X, Guan J, Chen X, Cui E, Li R *et al*: **Preoperative prediction of lymphovascular invasion in invasive breast cancer with dynamic contrast-enhanced-MRI-based radiomics.** *J Magn Reson Imaging* 2019, **50**(3):847-857.
29. Nakano K, Miki Y, Hata S, Ebata A, Takagi K, McNamara KM, Sakurai M, Masuda M, Hirakawa H, Ishida T *et al*: **Identification of androgen-responsive microRNAs and androgen-related genes in breast cancer.** *Anticancer research* 2013, **33**(11):4811-4819.
30. Sun Q, Zhang J, Cao W, Wang X, Xu Q, Yan M, Wu X, Chen W: **Dysregulated miR-363 affects head and neck cancer invasion and metastasis by targeting podoplanin.** *The international journal of biochemistry & cell biology* 2013, **45**(3):513-520.
31. Khuu C, Sehic A, Eide L, Osmundsen H: **Anti-proliferative Properties of miR-20b and miR-363 from the miR-106a-363 Cluster on Human Carcinoma Cells.** *MicroRNA (Sharjah, United Arab Emirates)* 2016, **5**(1):19-35.
32. Klintman M, Nilsson F, Bendahl PO, Fernö M, Liljegren G, Emdin S, Malmström P: **A prospective, multicenter validation study of a prognostic index composed of S-phase fraction, progesterone receptor status, and tumour size predicts survival in node-negative breast cancer patients: NNBC, the node-negative breast cancer trial.** *Annals of oncology : official journal of the European Society for Medical Oncology* 2013, **24**(9):2284-2291.
33. Costa A, Afonso J, Osório C, Gomes AL, Caiado F, Valente J, Aguiar SI, Pinto F, Ramirez M, Dias S: **miR-363-5p regulates endothelial cell properties and their communication with hematopoietic precursor cells.** *J Hematol Oncol* 2013, **6**(1):87.
34. Jechlinger M, Sommer A, Moriggl R, Seither P, Kraut N, Capodiecci P, Donovan M, Cordon-Cardo C, Beug H, Grunert S: **Autocrine PDGFR signaling promotes mammary cancer metastasis.** *J Clin Invest* 2006, **116**(6):1561-1570.
35. Donnem T, Al-Saad S, Al-Shibli K, Busund LT, Bremnes RM: **Co-expression of PDGF-B and VEGFR-3 strongly correlates with lymph node metastasis and poor survival in non-small-cell lung cancer.** *Ann Oncol* 2010, **21**(2):223-231.
36. Cao R, Bjorndahl MA, Religa P, Clasper S, Garvin S, Galter D, Meister B, Ikomi F, Tritsarlis K, Dissing S *et al*: **PDGF-BB induces intratumoral lymphangiogenesis and promotes lymphatic metastasis.** *Cancer Cell* 2004, **6**(4):333-345.

37. Schito L, Rey S, Tafani M, Zhang H, Wong CC, Russo A, Russo MA, Semenza GL: **Hypoxia-inducible factor 1-dependent expression of platelet-derived growth factor B promotes lymphatic metastasis of hypoxic breast cancer cells.** *Proc Natl Acad Sci U S A* 2012, **109**(40):E2707-2716.

Declarations

Ethics approval and consent to participate

All participants signed written informed consent. Ethics approval for the study was obtained from the Research Ethics Committee of CHCAMS. (reference number: NCC2017G-075).

Consent for publication

Not applicable.

Availability of data and materials

The datasets generated during the current study are not publicly available as the informed consent does not cover open data disclosure. The access to the data are available from the corresponding author on reasonable request according to approval from ethical and data protection board.

Competing interests

The authors declare that they have no competing interests.

Funding

This research was funded in part by the National Natural Science Foundation of China (81802669 to J.L.) and the CAMS Initiative Fund for Medical Sciences (2016-I2M-1-001 to Xiang Wang and 2017-I2M-3-004 to Xin Wang).

Authors' Contributions

Xin W established the study concept and coordinated laboratory assays. TQ wrote the manuscript with the support from Xin W, HC, JL and MZ. SB performed bioinformatic analysis, together with HZ. HC supervised laboratory assays. ZX, YL, MZ, XM, CW, JW and HG performed and supervised sample collection. JL coordinated the research. MZ and Xiang W contributed to the design and implementation of the research. All authors contributed to data interpretation and read and approved the final manuscript.

Acknowledgments

We thank all the individuals, families, and physicians involved in the study for their participation. We thank the nurses from the department of breast surgical oncology of CHCAMS for assistance with patient enrollment. We thank Echo Biotech Co., Ltd at Beijing, P. R. China for plasma Exosome RNAseq, helpful discussions and bioinformatic analysis.

Authors' information

Xin Wang, Tianyi Qian and Siqi Bao contributed equally to the study.

Department of Breast Surgical Oncology, National Cancer Center /National Clinical Research Center for Cancer/Cancer Hospital, Chinese Academy of Medical Sciences and Peking Union Medical College, Beijing 100021, China.

Xin Wang, Tianyi Qian, Zeyu Xing, Menglu Zhang, Xiangzhi Meng, Changchang Wang, Jie Wang, Hongxia Gao, Jiaqi Liu & Xiang Wang

School of Biomedical Engineering, Wenzhou Medical University, Wenzhou 325027, China.

Siqi Bao & Meng Zhou

Department of Orthopedic Surgery, Peking Union Medical College Hospital, Peking Union Medical College and Chinese Academy of Medical Sciences, Beijing 100021, China.

Hengqiang Zhao

State Key Laboratory of Molecular Oncology, National Cancer Center/National Clinical Research Center for Cancer/Cancer Hospital, Chinese Academy of Medical Sciences and Peking Union Medical College, Beijing 100021, China.

Hongyan Chen

Department of Breast Surgery, the Affiliated Yantai Yuhuangding Hospital of Qingdao University, Yantai 264000, China.

Yalun Li

Supplementary Information

Additional file 1: Fig.S1.pdf

Characterization of exosomes from the serum of breast cancer patients.

(A) TEM displayed a cup-shaped exosome. Scale bar 200nm. (B) Exosome markers confirmed by Western blot indicating the presence of TSG101 and CD63 but the absence of Calnexin. (C) NTA analysis revealed a main peak of 85.5nm.

Table

Table 1. The Clinical Information of the Patients in this Study

Patient	Gender	Age at diagnosis	Histology	T stage	N stage	M stage	Stage	Lymph node
A07-05	F	63	IDC	1c	1a	0	IIA	1/22
A07-07	F	49	IDC	1b	2a	0	IIA	2/24
A07-08	F	53	IDC	1c	0(sn)	0	IA	0/6
A07-09	F	67	IDC	2	0(sn)	0	IIA	0/5
A07-10	F	38	IDC	2	0(sn)	0	IIA	0/5
A07-11	F	55	DCIS	is	0(sn)	0	0	0/4
A07-12	F	57	IDC	1b	1a	0	IIA	1/23
A07-14	F	59	IDC	1c	0(sn)	0	IA	0/5
A07-17	F	64	IDC	2	0(sn)	0	IIA	0/6
A07-18	F	44	IDC	1c	1a	0	IIA	1/24

All patients were pathologically diagnosed with stage I-II IDC or DCIS, according to the breast cancer TNM anatomic stage classification from AJCC UICC (8th edition). IDC: invasive ductal carcinoma; DCIS: ductal carcinoma *in situ*.

Figures

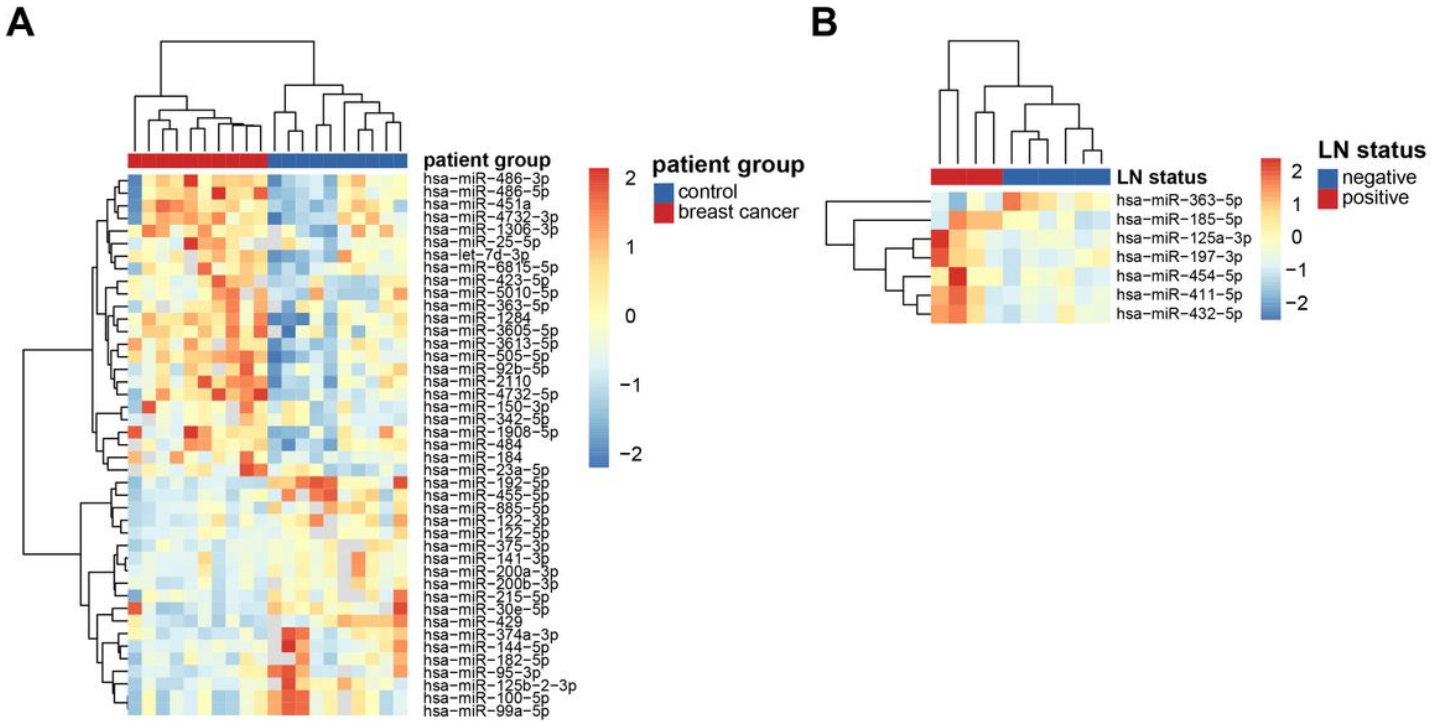


Figure 1

Differentially-expressed miRNAs in serum exosomes from breast cancer patients. Cluster analysis of exosomal miRNAs among (A) breast cancer patients and healthy individuals; (B) breast cancer patients with positive LN and negative LN. $p < 0.05$ determined by Student's t test

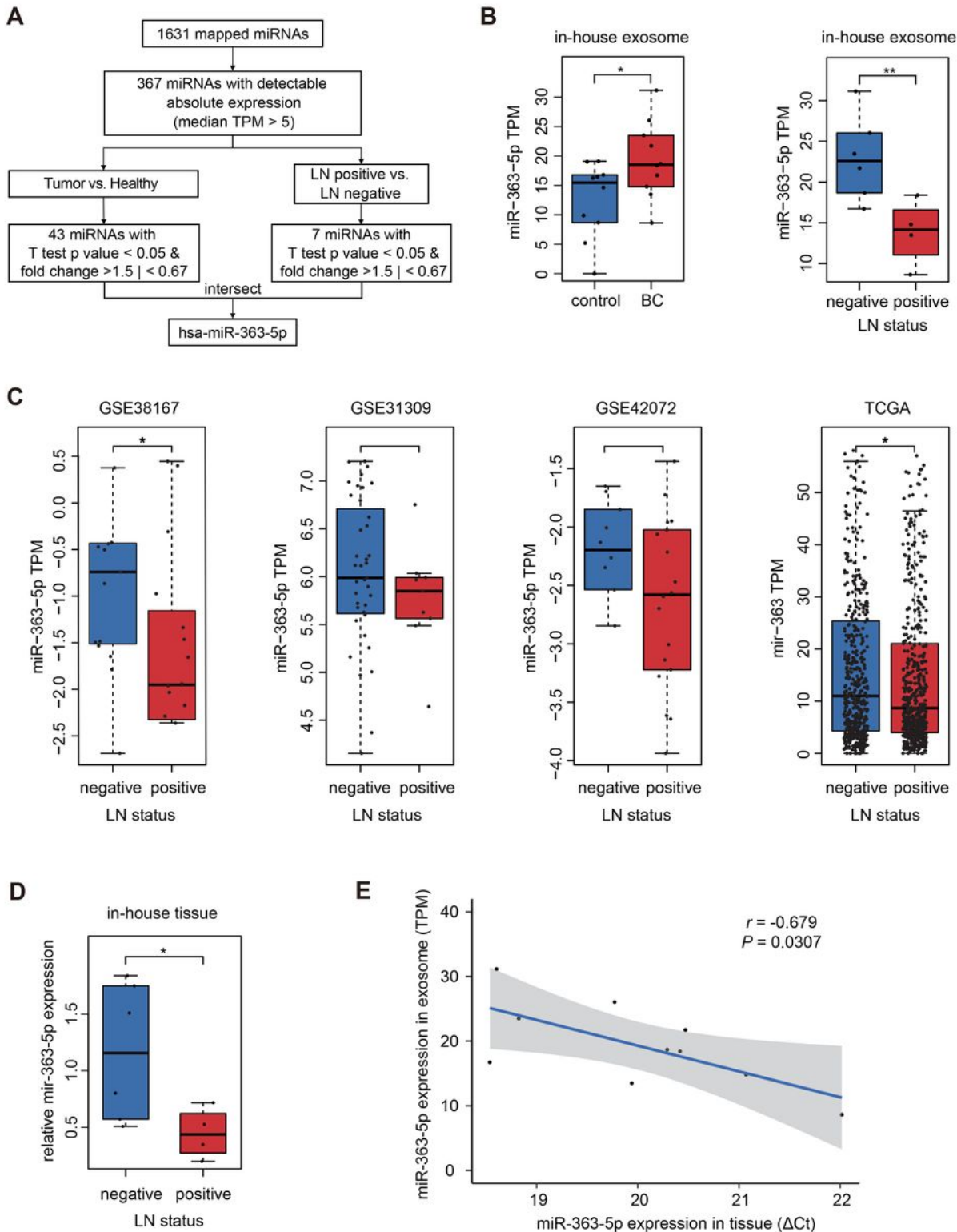


Figure 2

miR-363-5p is down-regulated in serum exosome and tumor tissue of breast cancer patients with positive LN (A) Workflow of the filtration procedures used in identifying the potential markers. (B) Exosomal miR-363-5p expression level of in-house data. (C) The presence of lymph node metastasis at diagnosis is associated with lower expression of miR-363-5p. Statistical significance was determined by the Mann-Whitney U test. (D) Tumors with positive ALN have significantly downregulated miR-363-5p. Expression

levels of miR-363-5p in breast cancer tissues were determined using qRT-PCR, * $p < 0.05$ by unpaired Student's t test. (E) The expression level of miR-363-5p in serum exosome correlates expression in tumor tissue. Pearson's correlation analysis was applied.

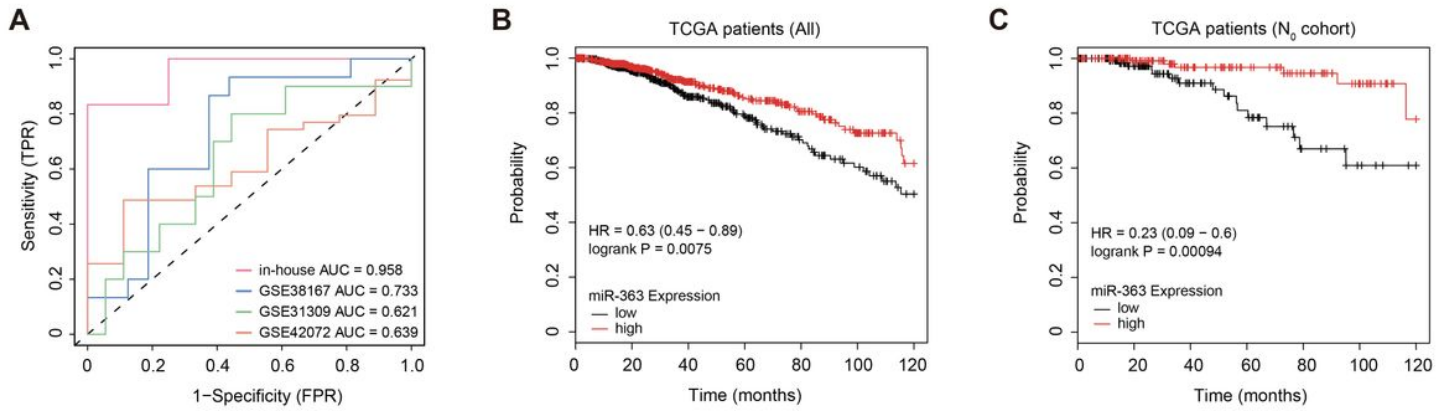
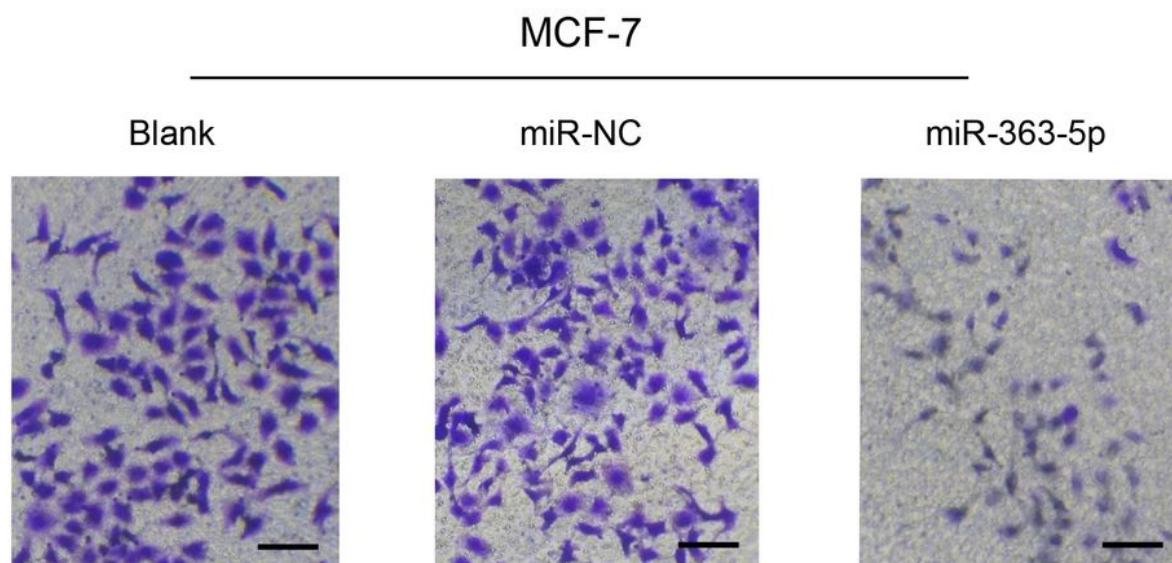
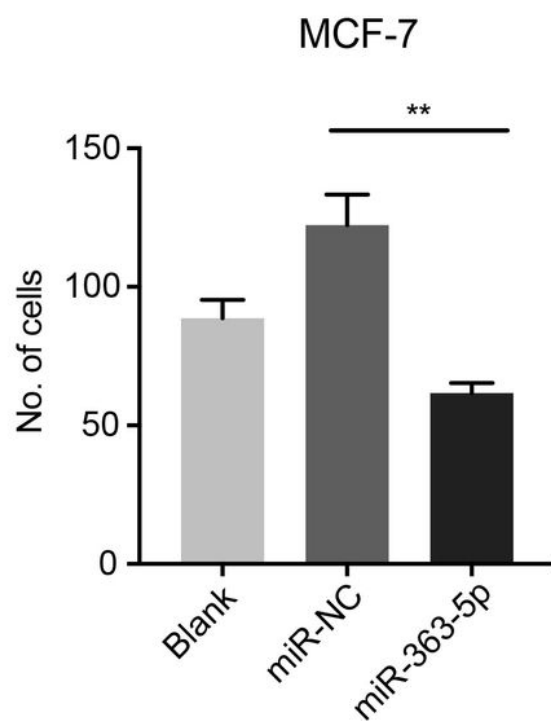
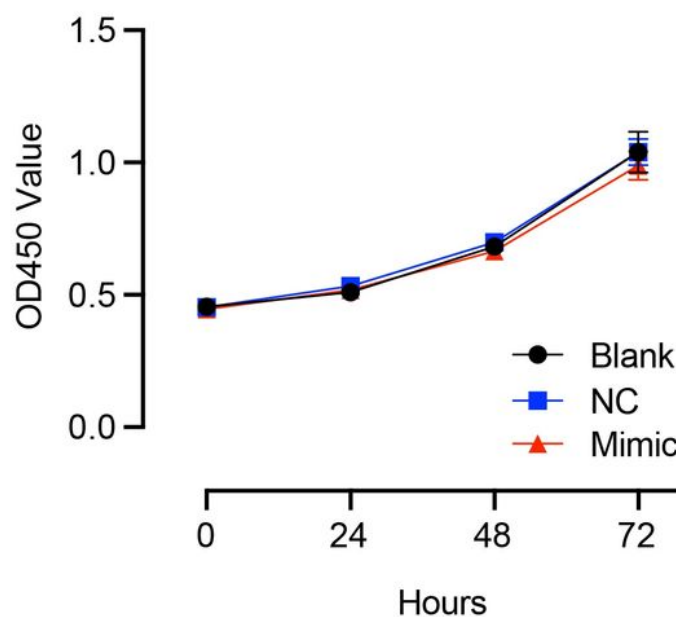


Figure 3

Performance evaluation verified miR-363-5p as LN metastasis and progression predictor (A) The ROC curve of the miR-363-5p for breast cancer LN metastasis. Kaplan-Meier survival analysis for all TCGA breast cancer patients (B) and patients with negative lymph nodes upon first diagnosis (C). Statistical significance was determined by the log-rank test.

A**B****C****Figure 4**

miR-363-5p inhibits metastatic properties of breast cancer cell (A and B) Migration assay of MCF-7 transfected miR-363-5p-mimic or normal control. Migrated cells were counted using Image J and representative images were shown. Scale bar, 20 μ m. Results are shown as mean \pm SE. Student's t test was used to analyze the data (* $p < 0.05$; ** $p < 0.01$). (C) Proliferation ability of MCF-7 transfected with miR-363-5p-mimic or normal control was determined by CCK-8 assay.

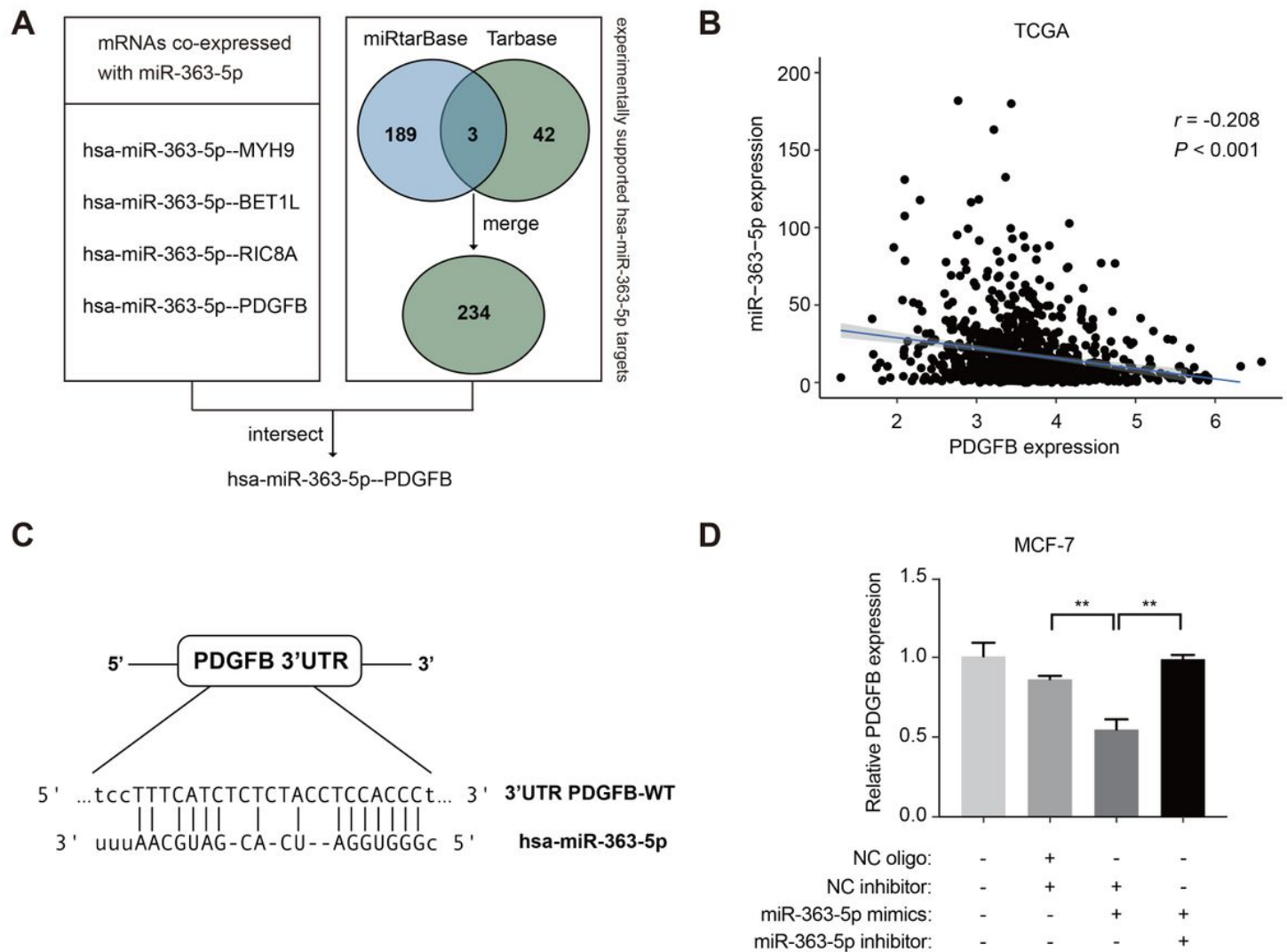


Figure 5

miR-363-5p suppresses PDGFB expression by binding to its 3'-UTR (A) The strategy applied in target identification. (B) A negative correlation between miR-363-5p expression and PDGFB mRNA levels in breast cancer tissues was analyzed using Pearson's correlation analysis. (C) miR-363-5p binding sequences in PDGFB 3'-UTR. (D) qRT-PCR assay of PDGFB expression level of MCF-7 transfected with miR-363-5p-mimic, miR-363-5p-inhibitor or normal control.

Supplementary Files

This is a list of supplementary files associated with this preprint. Click to download.

- [Fig.S1.pdf](#)